

Forced Vibration Analysis in Axisymmetric Functionally Graded Viscothermoelastic Hollow Cylinder Under Dynamic Pressure

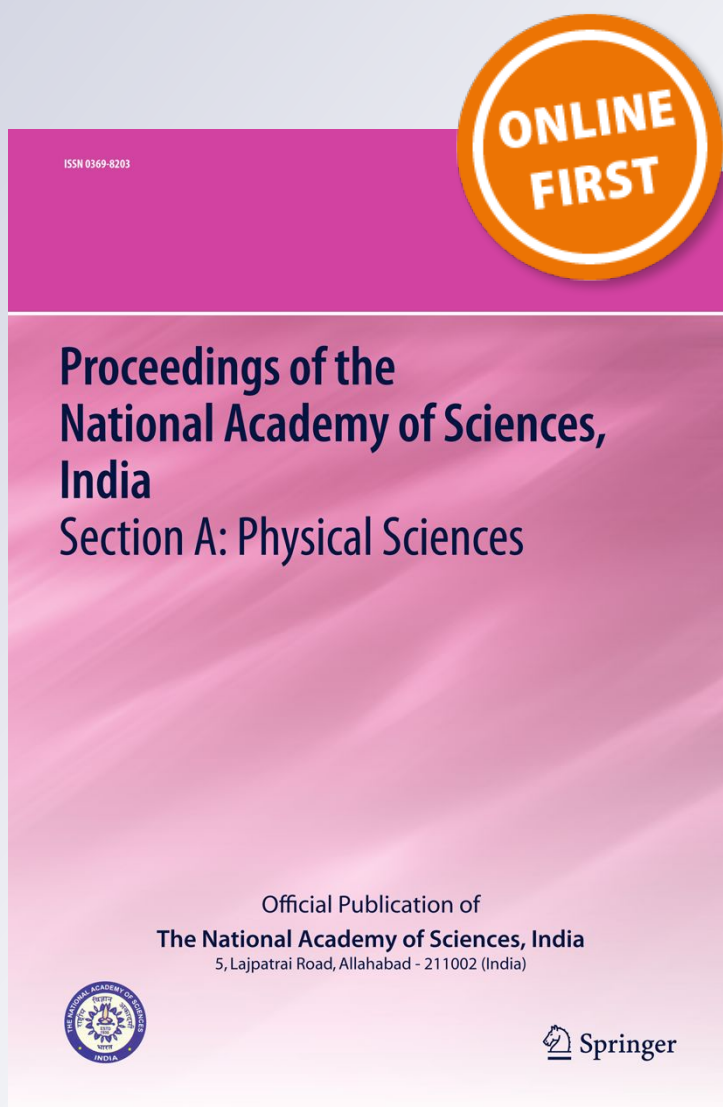
Dinesh Kumar Sharma, Himani Mittal & Sita Ram Sharma

Proceedings of the National Academy of Sciences, India Section A: Physical Sciences

ISSN 0369-8203

Proc. Natl. Acad. Sci., India, Sect. A Phys. Sci.

DOI 10.1007/s40010-019-00634-3



Your article is protected by copyright and all rights are held exclusively by The National Academy of Sciences, India. This e-offprint is for personal use only and shall not be self-archived in electronic repositories. If you wish to self-archive your article, please use the accepted manuscript version for posting on your own website. You may further deposit the accepted manuscript version in any repository, provided it is only made publicly available 12 months after official publication or later and provided acknowledgement is given to the original source of publication and a link is inserted to the published article on Springer's website. The link must be accompanied by the following text: "The final publication is available at link.springer.com".



Forced Vibration Analysis in Axisymmetric Functionally Graded Viscothermoelastic Hollow Cylinder Under Dynamic Pressure

Dinesh Kumar Sharma¹ · Himani Mittal¹ · Sita Ram Sharma²Received: 24 April 2018 / Revised: 8 July 2019 / Accepted: 11 July 2019
© The National Academy of Sciences, India 2019

Abstract The forced vibrations of axisymmetric inhomogeneous isotropic viscothermoelastic hollow cylinder under periodic dynamic pressure have been studied. The material was taken inhomogeneous due to easy exponent law in radial direction. By applying time harmonics variation technique, the partial differential equations were converted into ordinary differential equations. These ordinary differential equations were solved by applying series solution of matrix Fröbenius method analytically to represent displacement, temperature and stresses. Numerically simulated outcomes were presented graphically to express the effect of functionally graded material disk for different values of grading parameter. With the increase in value of grading index, variation of field functions go on decreasing. The variation of field functions show high variation in homogeneous materials in contrast to low variation in inhomogeneous materials.

Keywords Forced vibrations · Dynamic pressure · Inhomogeneous · Fröbenius method · De-hoop stress

✉ Dinesh Kumar Sharma
dksharma200513@gmail.com

Himani Mittal
himanimittal9@gmail.com

Sita Ram Sharma
sita.ram@chitkarauniversity.edu.in

¹ Department of Mathematics, School of Basic and Applied Sciences, Maharaja Agrasen University, Baddi, District Solan, HP 174103, India

² Chitkara University School of Engineering and Technology, Chitkara University, Baddi, District Solan, HP 174103, India

1 Introduction

Functionally graded materials (FGMs) also known as graded materials are generally many-sided phase composites having continuously changing properties. Depending on the positions of the material, the properties of these materials are not uniformly distributed across the whole material. Chen [1] had studied the problem of elastic medium based on spherically isotropic material bounded by two concentric spherical surfaces. Honarvar and Sinclair [2] have derived mathematical expressions for plane acoustic waves in transversely isotropic elastic cylinder. Dai et al. [3] presented numerical method to analyze the elasto-thermodynamic long hollow cylinder prepared by functionally graded materials in radial direction under symmetric mechanical and thermal loads. Keles and Tutuncu [4] have studied the free and forced vibration analysis of functionally graded transversely isotropic elastic hollow cylinder in radial direction by using easy exponent law and represented the stresses, displacements and temperatures under dynamic loads. Othman et al. [5] have presented a mathematical model based on normal mode analysis in which two-dimensional viscothermoelastic (VTE) problem has been investigated in the medium with two relaxation time parameters for the temperature distribution, thermal stresses and the displacement components.

Flugge [6] and Hunter [7] have done mathematical models in which they utilize the dissipation factor caused by internal energy in the vibrating viscoelastic solids. Lord and Shulman [8] have modified Fourier law of heat conduction to acquire a hyperbolic equation that confesses a finite speed of thermal signals where Green and Lindsay [9] have demonstrated that second sound effects are short lived and is based on the entropy production inequality.

Sharma and Othman [10] have studied the effect of rotation in thermoelastic plate of infinite Kelvin–Voigt viscoelastic (VE) model for coupled and generalized theories of thermoelasticity. Sharma et al. [11] presented the frequency shift and thermoelastic damping for vibration modes in transversely isotropic solid cylinder in the context of coupled thermoelasticity. Sharma et al. [12] studied thermoelasto-diffusion dynamic problem for infinite cylindrical cavity and displayed analytical and graphical distributions of displacement, temperature, concentration and stress. Sharma et al. [13, 14] studied frequency vibrations and damping in three-dimensional stress-free and rigidly fixed vibrations for a homogenous isotropic, generalized viscothermoelastic hollow sphere. Sharma et al. [15] studied the free vibrations of Lord and Shulman theory of generalized thermoelasticity in transversely isotropic inhomogeneous thermoelastic (TE) cylinder. Sharma et al. [16] studied the generalized stress-free viscothermoelastic hollow sphere and presented graphically the natural frequency, thermoelastic damping, frequency shift, temperature, displacement and stresses.

Xin et al. [17] have studied the effect of volume fraction and Poisson’s ratio as well as ratio of two Young’s moduli on the radial displacement and stresses of functionally graded thick-walled tube subjected to internal pressure. Xin et al. [18] discussed the problem of thermoelastic functionally graded thick-walled tube based on axisymmetric mechanical and thermal loads and presented the effect on Poisson’s ratio of two thermal conduction coefficients on displacement and stresses. Tripathi et al. [19] investigated the effect of axisymmetric heat supply on thick plate of infinite extent in the context of diffusion thermoelasticity (TE). Khanna and Kaur [20] have analyzed coupling problem of non-homogenous viscoelastic rectangular plate with bipolar temperature variation with the help of Rayleigh–Ritz approach. Sharma et al. [21] studied the dynamic response of functionally graded transversely isotropic thermoelastic cylinders under time-dependent heat flux. Xin et al. [22] described the elastic plastic problem of thick-walled functionally graded tube subjected to internal pressure on stresses and displacements and provided the solutions in terms of volume fractions. Sharma [23] studied the viscothermoelastic waves of homogenous isotropic spherical curved plates and presented toroidal and spheroidal vibrations graphically. Sharma [24] has presented the propagation of circumferential thermoelastic waves of homogenous transversely and circumferential curved plates. Xin et al. [25] presented thick-walled tube based on Voigt method and also studied the transversely isotropic inhomogeneous tube to produce the results for radial displacement and stresses by using Mori–Tanaka method. Tomantschger [26] has explained the series solutions method for resolving coupled system of differential

equations in which one regular singular point involved to explain the performance of micropolar suspension among two coaxial cylinders. Cullen [27] has developed the procedure of convergence of matrix equations obtained from series solution. Pierce [28] has applied normal mode analysis to solve nonlinear differential equations. Dhaliwal and Singh [29] have solved the elastic and thermoelastic problems. Neuringer [30] developed the procedure of series solution of Fröbenius method when indicial equation gave complex roots.

Here, we present exact vibration analysis of inhomogeneous isotropic viscothermoelastic hollow cylinder based on mechanical periodic-loaded boundary conditions under dynamic pressure. The analytical and numerical results such as displacement, temperature change and stresses against time and normalized thickness are presented graphically.

2 Formation of the Mathematical Model

We assume a thermally conducting functionally graded axisymmetric isotropic viscothermoelastic hollow cylinder/disk with domain $a \leq r \leq \xi a$ of outer radius and inner radius ξa and a , respectively, initially at uniform temperature T_0 . The components of displacement in cylindrically coordinated system (r, ϑ, z) are expressed as $u_\vartheta = u_z = 0$ and $u_r = u(r, t)$, respectively. The viscothermoelastic hollow cylinder having governing equations of motion and heat conduction for isotropic medium of inner radius a and outer radius ξa in the absence of body forces and heat sources are given by Dai et al. [3] and Dhaliwal and Singh [29] as:

$$\frac{\partial \sigma_{rr}}{\partial r} + \frac{1}{r}(\sigma_{rr} - \sigma_{\vartheta\vartheta}) = \rho \frac{\partial^2 u}{\partial t^2} \tag{1}$$

$$\begin{aligned} \frac{1}{r} \frac{\partial}{\partial r} \left(Kr \frac{\partial T}{\partial r} \right) - \rho C_e \left(\frac{\partial}{\partial t} + t_0 \frac{\partial^2}{\partial t^2} \right) T \\ = T_0 \beta^* \left(\frac{\partial}{\partial t} + t_0 \delta_{1k} \frac{\partial^2}{\partial t^2} \right) (e_{rr} + e_{\vartheta\vartheta}) \end{aligned} \tag{2}$$

where stress–strain–temperature and strain–displacement relations are:

$$\begin{pmatrix} \sigma_{rr} \\ \sigma_{\vartheta\vartheta} \end{pmatrix} = \begin{pmatrix} \lambda^* + 2\mu^* & \lambda^* \\ \lambda^* & \lambda^* + 2\mu^* \end{pmatrix} \begin{pmatrix} e_{rr} \\ e_{\vartheta\vartheta} \end{pmatrix} - \beta^* \begin{pmatrix} T + t_1 \delta_{2k} \dot{T} \\ T + t_1 \delta_{2k} \dot{T} \end{pmatrix} \tag{3}$$

$$e_{rr} = \frac{\partial u}{\partial r}, \quad e_{\vartheta\vartheta} = \frac{u}{r}, \tag{4}$$

Here σ_{ij} and e_{ij} ; $(i, j = r, \vartheta)$ are stress and strain components, respectively; $\vec{u} = u(r, t)$ and $T(r, t)$ are the displacement and temperature, respectively; ρ, K and C_e are mass density,

thermal conductivity and specific heat at constant strain, respectively. t_0 and t_1 are the thermal relaxation time parameters and $\beta^* = (3\lambda^* + 2\mu^*)\alpha_T$ is the viscothermoelastic coupling constant. λ^* and μ^* are viscoelastic parameters; the quantity δ_{ik} , ($i = 1, 2$) is the Kronecker's delta in which $k = 1$ and $k = 2$ are taken for Lord–Shulman (LS) and Green–Lindsay (GL) theories, respectively. The thermal conductivity, density, modulus of viscoelasticity and viscothermoelasticity of the material have been assumed to vary with the radial coordinate according to exponent law as under:

$$(\lambda^*, \mu^*, \beta^*, \rho, K) = (\lambda_0, \mu_0, \beta_0^*, \rho_e, K_0) \left(\frac{r}{a}\right)^\gamma \tag{5}$$

where the exponent γ is the degree of inhomogeneity and $\lambda_0, \mu_0, \beta_0^*, \rho_e, K_0$ are the homogenous components of respective quantities. The parameters of the material have been defined as:

$$\lambda_0 = \lambda_e \left(1 + \alpha_0 \frac{\partial}{\partial t}\right), \quad \mu_0 = \mu_e \left(1 + \alpha_1 \frac{\partial}{\partial t}\right), \tag{6}$$

$$\beta_0^* = \beta_e \left(1 + \beta_0 \frac{\partial}{\partial t}\right)$$

$$\beta_e = (3\lambda_e + 2\mu_e)\alpha_T, \quad \beta_0 = \left(\frac{(3\lambda_e\alpha_0 + 2\mu_e\alpha_1)\alpha_T}{\beta_e}\right)$$

The quantities λ_e, μ_e and α_0, α_1 are Lamé's parameters and viscoelastic relaxation times; α_T is the coefficient of linear thermal expansion of the material.

Substituting Eqs. (5)–(6) via Eqs. (3)–(4) in Eqs. (1)–(2), we obtain:

$$\frac{\beta_e}{(\lambda_e + 2\mu_e)} \left(1 + \beta_0 \frac{\partial}{\partial t}\right) \left(1 + t_1 \delta_{2k} \frac{\partial}{\partial t}\right) \left(\frac{\partial T}{\partial r} + \frac{\gamma}{r} T\right) - \left\{ \left(1 + \delta_0 \frac{\partial}{\partial t}\right) \left(\frac{\partial^2 u}{\partial r^2} + \frac{m_1}{r} \frac{\partial u}{\partial r}\right) + \frac{m'_2}{r^2} u \right\} = \frac{\rho_e}{(\lambda_e + 2\mu_e)} \frac{\partial^2 u}{\partial t^2} \tag{7}$$

$$\left(1 + \beta_0 \frac{\partial}{\partial t}\right) \left(\frac{\partial}{\partial t} + t_0 \delta_{1k} \frac{\partial^2}{\partial t^2}\right) \left(\frac{\partial u}{\partial r} + \frac{1}{r} u\right) = \frac{K_0}{T_0 \beta_e} \left\{ \frac{\partial^2 T}{\partial r^2} + \frac{m_1}{r} \frac{\partial T}{\partial r} \right\} - \frac{\rho_e C_e}{T_0 \beta_e} \left(\frac{\partial}{\partial t} + t_0 \frac{\partial^2}{\partial t^2}\right) T \tag{8}$$

$$\begin{pmatrix} \sigma_{rr} \\ \sigma_{\theta\theta} \end{pmatrix} = (\lambda_0 + 2\mu_0) \left(\frac{r}{a}\right)^\gamma \left\{ \begin{pmatrix} 1 & \frac{\lambda_0}{(\lambda_0 + 2\mu_0)} \\ \frac{\lambda_0}{(\lambda_0 + 2\mu_0)} & 1 \end{pmatrix} \begin{pmatrix} e_{rr} \\ e_{\theta\theta} \end{pmatrix} - \frac{\beta_0^*}{(\lambda_0 + 2\mu_0)} \begin{pmatrix} T + t_1 \delta_{2k} \dot{T} \\ T + t_1 \delta_{2k} \dot{T} \end{pmatrix} \right\} \tag{9}$$

where $m_1 = \gamma + 1, m'_2 = -\left(1 - \gamma \frac{\lambda_0}{\lambda_0 + 2\mu_0}\right),$

We introduce the following quantities to remove the complexity of above equations:

$$\bar{\varepsilon} = \frac{T_0 \beta_e}{(\lambda_e + 2\mu_e)}, \quad \varepsilon_T = \frac{T_0 \beta_e^2}{\rho_e C_e (\lambda_e + 2\mu_e)}, \quad x = \frac{r}{a},$$

$$\tau = \frac{c_1 t}{a}, \quad w = \frac{u}{a}, \quad \theta = \frac{T}{T_0}, \quad \left(\hat{\alpha}_0, \hat{\alpha}_1 = \frac{c_1}{a} (\alpha_0, \alpha_1)\right)$$

$$\hat{\beta}_0 = \frac{c_1}{a} \beta_0, \quad \Omega^* = \frac{a \omega^*}{c_1}, \quad \tau_{xx} = \frac{\sigma_{rr}}{\rho_e c_1^2}, \quad \tau_{\theta\theta} = \frac{\sigma_{\theta\theta}}{\rho_e c_1^2},$$

$$\delta_0 = \hat{\alpha}_0 + 2\delta^2 (\hat{\alpha}_1 - \hat{\alpha}_0), \quad \delta^2 = \frac{c_2^2}{c_1^2},$$

$$\tau_0 = \frac{c_1}{a} t_0, \quad \tau'_0 = \frac{c_1}{a} t'_0, \quad \tau_1 = \frac{c_1}{a} t_1, \quad \omega^* = \frac{C_e (\lambda_e + 2\mu_e)}{K_0},$$

$$c_1^2 = \frac{(\lambda_e + 2\mu_e)}{\rho_e}, \quad c_2^2 = \frac{\mu_e}{\rho_e}, \tag{10}$$

Here ω^* is characteristic frequency, c_1 and c_2 are shear and longitudinal wave velocities, respectively. Using non-dimensional quantities from Eq. (10) in Eqs. (7) to (9), we obtain:

$$\left(1 + \delta_0 \frac{\partial}{\partial \tau}\right) \left(\frac{\partial^2 w}{\partial x^2} + \frac{m_1}{x} \frac{\partial w}{\partial x}\right) + \frac{m'_2}{x^2} w - \frac{\partial^2 w}{\partial \tau^2} = \bar{\varepsilon} \left(1 + \hat{\beta}_0 \frac{\partial}{\partial \tau}\right) \left(1 + \tau_1 \delta_{2k} \frac{\partial}{\partial \tau}\right) \left(\frac{\partial \theta}{\partial x} + \frac{\gamma}{x} \theta\right) \tag{11}$$

$$\frac{\partial^2 \theta}{\partial x^2} + \frac{m_1}{x} \frac{\partial \theta}{\partial x} - \Omega^* \left(\frac{\partial}{\partial \tau} + \tau_0 \frac{\partial^2}{\partial \tau^2}\right) \theta = \varepsilon_T \frac{\Omega^*}{\bar{\varepsilon}} \left(1 + \hat{\beta}_0 \frac{\partial}{\partial \tau}\right) \left(\frac{\partial}{\partial \tau} + \tau'_0 \delta_{1k} \frac{\partial^2}{\partial \tau^2}\right) \left(\frac{\partial w}{\partial x} + \frac{w}{x}\right) \tag{12}$$

$$\begin{pmatrix} \tau_{xx} \\ \tau_{\theta\theta} \end{pmatrix} = x^\gamma \begin{pmatrix} \left(1 + \delta_0 \frac{\partial}{\partial \tau}\right) & h \left(1 + \hat{\alpha}_0 \frac{\partial}{\partial \tau}\right) & -\bar{\varepsilon} \left(1 + \hat{\beta}_0 \frac{\partial}{\partial \tau}\right) \left(1 + \tau_1 \frac{\partial}{\partial \tau}\right) \\ h \left(1 + \hat{\alpha}_0 \frac{\partial}{\partial \tau}\right) & \left(1 + \delta_0 \frac{\partial}{\partial \tau}\right) & -\bar{\varepsilon} \left(1 + \hat{\beta}_0 \frac{\partial}{\partial \tau}\right) \left(1 + \tau_1 \frac{\partial}{\partial \tau}\right) \end{pmatrix} \begin{pmatrix} \frac{\partial w}{\partial x} \\ \frac{w}{x} \\ \theta \end{pmatrix} \tag{13}$$

where $m'_2 = (\gamma h (1 + \hat{\alpha}_0 \frac{\partial}{\partial \tau}) - (1 + \delta_0 \frac{\partial}{\partial \tau})), \quad h = (1 - 2\delta^2).$

3 Initial and Regular Boundary Conditions

The medium has been considered undisturbed both mechanically and thermally to be at rest and at initial time, the non-dimensional initial conditions are given as:

$$w(r, 0) = 0 = \frac{\partial w(r, 0)}{\partial \tau}, \theta(r, 0) = 0 = \frac{\partial \theta(r, 0)}{\partial \tau}, \quad (14)$$

at $r = a, \xi a$

The outer surface $r = \xi a$ of functionally graded hollow cylinder has been assumed traction-free mechanically i.e. $(\sigma_{rr} = 0)$ and isothermal $(T = 0)$ conditions in dimensional form. Mathematically, the respective boundary conditions in non-dimensional form at $x = \xi$ provide us:

$$\begin{aligned} & \left(1 + \delta_0 \frac{\partial}{\partial \tau}\right) \frac{\partial w}{\partial x} + (1 - 2\delta^2) \left(1 + \hat{\alpha}_0 \frac{\partial}{\partial \tau}\right) \frac{w}{x} \\ & - \bar{\varepsilon} \left(1 + \hat{\beta}_0 \frac{\partial}{\partial \tau}\right) \left(1 + \tau_1 \frac{\partial}{\partial \tau}\right) \theta = 0, \quad \theta = 0 \end{aligned} \quad (15)$$

While calculating subject to the conditions in Eq. (15), the dynamic pressure $(\sigma_{rr} = -Q(t))$ has been applied to inner surface of the boundary $(r = a)$ of hollow cylinder (disk) which is assumed to be thermally insulated $(\frac{\partial T}{\partial r} = 0)$ in dimensional form. Therefore, mathematically the boundary conditions in non-dimensional form at $x = 1$ give us:

$$\begin{aligned} & \left(1 + \delta_0 \frac{\partial}{\partial \tau}\right) \frac{\partial w}{\partial x} + (1 - 2\delta^2) \left(1 + \hat{\alpha}_0 \frac{\partial}{\partial \tau}\right) \frac{w}{x} \\ & - \bar{\varepsilon} \left(1 + \hat{\beta}_0 \frac{\partial}{\partial \tau}\right) \left(1 + \tau_1 \frac{\partial}{\partial \tau}\right) \theta = -Q(\tau) \end{aligned} \quad (16)$$

$$\frac{\partial \theta}{\partial x} = 0$$

The governing Eqs. (11)–(16) represent the mathematical model of this problem.

4 Solution of the Mathematical Model

Here we apply time harmonic vibrations as used by Pierce [28], we have:

$$\begin{aligned} w(x, \tau) &= \bar{w}(x, \tau) \exp(i\Omega\tau) \\ \theta(x, \tau) &= \bar{\theta}(x, \tau) \exp(i\Omega\tau) \end{aligned} \quad (17)$$

where $\Omega = \frac{\omega a}{c_1}$, is non-dimensional circular frequency of vibrations. Substituting Eq. (17) in Eqs. (11)–(13), we obtain:

$$\begin{pmatrix} \nabla_1^2 + \left(\frac{m_2}{x^2} + \frac{i\Omega}{\tilde{\delta}_0}\right) & i\Omega m_3 \left(\frac{d}{dx} + \frac{\gamma}{x}\right) \\ i\Omega^3 m_4 \left(\frac{d}{dx} + \frac{1}{x}\right) & (\nabla_1^2 - \Omega^* \Omega^2 \tilde{\tau}_0) \end{pmatrix} \begin{pmatrix} \bar{w} \\ \bar{\theta} \end{pmatrix} = \begin{pmatrix} 0 \\ 0 \end{pmatrix} \quad (18)$$

$$\begin{pmatrix} \tau_{xx} \\ \tau_{\theta\theta} \end{pmatrix} = -i\Omega x^\gamma \begin{pmatrix} \tilde{\delta}_0 \frac{d}{dx} & h\tilde{\alpha}_0 & i\Omega \tilde{\varepsilon} \tilde{\beta}_0 \tilde{\tau}_1 \\ h\tilde{\alpha}_0 \frac{d}{dx} & \tilde{\delta}_0 & i\Omega \tilde{\varepsilon} \tilde{\beta}_0 \tilde{\tau}_1 \end{pmatrix} \begin{pmatrix} \bar{w} \\ \bar{w}/x \\ \bar{\theta} \end{pmatrix} \quad (19)$$

where

$$\begin{aligned} m_2 &= \left(\frac{\hbar}{\tilde{\delta}_0} \gamma \tilde{\alpha}_0 - 1\right), \quad \tilde{\alpha}_0 = i\Omega^{-1} - \hat{\alpha}_0, \quad \tilde{\alpha}_1 = i\Omega^{-1} - \hat{\alpha}_1, \\ \tilde{\beta}_0 &= i\Omega^{-1} - \hat{\beta}_0, \quad \tilde{\delta}_0 = i\Omega^{-1} - \delta_0, \quad \tilde{\tau}_1 = i\Omega^{-1} - \tau_1, \\ \tilde{\tau}_0 &= i\Omega^{-1} - \tau_0, \\ \tau'_0 &= i\Omega^{-1} - \tau'_0, \quad \nabla_1^2 = \frac{d^2}{dx^2} + \frac{m_1}{x} \frac{d}{dx}, \quad m_3 = \frac{\tilde{\varepsilon} \tilde{\beta}_0 \tilde{\tau}_1}{\tilde{\delta}_0}, \\ m_4 &= \frac{\varepsilon T}{\varepsilon} \Omega^* \tilde{\beta}_0 \tilde{\tau}'_0 \end{aligned} \quad (20)$$

We introduce transformation defined by Sharma et al. [15] as:

$$\begin{aligned} \bar{w}(x, \tau) &= x^{-\frac{\gamma}{2}} v(x, \tau) \\ \bar{\theta}(x, \tau) &= x^{-\frac{\gamma}{2}} \Theta(x, \tau) \end{aligned} \quad (21)$$

Using transformation from Eq. (21) in Eqs. (18)–(19) and after simplifications, we get:

$$\begin{aligned} & \nabla^2 \begin{pmatrix} 1 & 0 \\ 0 & 1 \end{pmatrix} \begin{pmatrix} v \\ \Theta \end{pmatrix} + i\Omega \begin{pmatrix} \frac{1}{\tilde{\delta}_0} & m_3 \frac{d}{dx} \\ \Omega^2 m_4 \frac{d}{dx} & i\Omega \Omega^* \tilde{\tau}_0 \end{pmatrix} \begin{pmatrix} v \\ \Theta \end{pmatrix} \\ & + \begin{pmatrix} -\frac{\eta^2}{x^2} & i\Omega m_3 \frac{\gamma}{2x} \\ i\Omega^3 m_4 \left(\frac{2-\gamma}{2x}\right) & -\frac{\gamma^2}{4x^2} \end{pmatrix} \begin{pmatrix} v \\ \Theta \end{pmatrix} \\ & = 0 \end{aligned} \quad (22)$$

$$\begin{pmatrix} \tau_{xx} \\ \tau_{\theta\theta} \end{pmatrix} = -i\Omega \tilde{\delta}_0 x^{-\frac{\gamma}{2}} \begin{pmatrix} \left(\frac{d}{dx} + \frac{m_5}{x}\right) & i\Omega m_3 \\ \frac{\tilde{\alpha}_0 \hbar}{\tilde{\delta}_0} \left(\frac{d}{dx} + \frac{m_6}{x}\right) & i\Omega m_3 \end{pmatrix} \begin{pmatrix} v \\ \Theta \end{pmatrix} \quad (23)$$

where $\eta^2 = \frac{\gamma^2}{4} - m_2$, $\nabla^2 = \frac{1}{x} \frac{d}{dx} \left(x \frac{d}{dx}\right)$, $m_5 = \frac{1}{\tilde{\delta}_0} (\hbar \tilde{\alpha}_0 - \frac{\gamma}{2})$, $m_6 = \left(\frac{\tilde{\delta}_0}{\hbar \tilde{\alpha}_0} - \frac{\gamma}{2}\right)$.

5 Power Series Solution

Here it is to be noted that $x = 0$ is a regular singular point in matrix differential Eq. (22), and it has at least one possible non-trivial solution as discussed by Tomantschger [26] so that, we use the series solution of matrix Fröbenius method:

$$\begin{pmatrix} v(x, \tau) \\ \Theta(x, \tau) \end{pmatrix} = \sum_{k=0}^{\infty} \begin{pmatrix} L_k(s) \\ M_k(s) \end{pmatrix} x^{s+k} \quad (24)$$

where s and $(L_k \ M_k)'$ are the real or complex eigen values and unknown coefficients are to be determined. The

considered domain of the problem is $a \leq r \leq \xi a$, $a > 0$, in dimensional form and hence the matrix differential Eq. (22) has domain $1 \leq x \leq \xi$ in non-dimensional form. Thus, the solution of Eq. (22) is appropriate in some interval $1 \leq x \leq R$, $R > \xi$ (about origin).

Substituting considered series solution (24) in matrix Eq. (22) and simplifying, we obtain:

$$\sum_{k=0}^{\infty} \left\{ \frac{1}{x^2} (g_1(s+k))_{2 \times 2} + \frac{1}{x} (g_2(s+k))_{2 \times 2} + (g)_{2 \times 2} \right\} \begin{pmatrix} L_k(s) \\ M_k(s) \end{pmatrix} x^{s+k} = 0 \tag{25}$$

where

$$g_1(s+k) = \begin{pmatrix} (s+k)^2 - \eta^2 & 0 \\ 0 & (s+k)^2 - \frac{\gamma^2}{4} \end{pmatrix},$$

$$g = \begin{pmatrix} \frac{i\Omega}{\tilde{\delta}_0} & 0 \\ 0 & -\Omega^* \Omega^2 \tilde{\tau}_0 \end{pmatrix}$$

$$g_2(s+k) = \begin{pmatrix} 0 & A^* \left(s+k + \frac{\gamma}{2} \right) \\ B^* \left(s+k + \frac{2-\gamma}{2} \right) & 0 \end{pmatrix},$$

$$A^* = i\Omega m_3, B^* = i\Omega^3 m_4 \tag{26}$$

Equating the lowest power coefficient of x ; (i.e. x^{s-2}) in Eq. (25) to zero, we get:

$$\begin{pmatrix} s^2 - \eta^2 & 0 \\ 0 & s^2 - \frac{\gamma^2}{4} \end{pmatrix} \begin{pmatrix} L_0(s) \\ M_0(s) \end{pmatrix} = \begin{pmatrix} 0 \\ 0 \end{pmatrix} \tag{27}$$

The matrix Eq. (27) has non-trivial solution if the determinant of matrix equals to zero and leads to following indicial equation:

$$s^4 - \left(\eta^2 + \frac{\gamma^2}{4} \right) s^2 + \frac{\eta^2 \gamma^2}{4} = 0 \tag{28}$$

The roots of indicial equation are:

$$s_1 = \eta, \quad s_2 = -\eta, \quad s_3 = \frac{\gamma}{2}, \quad s_4 = -\frac{\gamma}{2} \tag{29}$$

This is to be noticed from above roots that s_1, s_2, s_3 and s_4 satisfy the property that $s_2 = -s_1$ and $s_4 = -s_3$. The roots s_1, s_2 are complex and s_3, s_4 are real. Thus, the leading term in the former case in series solution (25) is of the type:

$$\begin{pmatrix} L_0(s_j) \\ M_0(s_j) \end{pmatrix} x^s = \begin{pmatrix} L_0(s_j) \\ M_0(s_j) \end{pmatrix} x^{s_R + i s_I}$$

$$= \begin{pmatrix} L_0(s_j) \\ M_0(s_j) \end{pmatrix} x^{s_R} (\cos(s_I \ln(x)) + \sin(s_I \ln(x))) \tag{30}$$

where s_R and s_I are real and imaginary parts of complex eigen values. Due to Neuringer [30], the sufficient use of any one of the complex root of indicial equation is to locate two independent real solutions of the system of matrix differential equation. For the choice of indicial equation roots from the system of matrix Eq. (27) the unknowns $L_0(s_j)$ and $M_0(s_j)$ are chosen as:

$$\begin{pmatrix} L_0(s_1) \\ M_0(s_1) \end{pmatrix} = \begin{pmatrix} 1 \\ 0 \end{pmatrix}, \begin{pmatrix} L_0(s_2) \\ M_0(s_2) \end{pmatrix} = \begin{pmatrix} 1 \\ 0 \end{pmatrix}, \begin{pmatrix} L_0(s_3) \\ M_0(s_3) \end{pmatrix} = \begin{pmatrix} 0 \\ 1 \end{pmatrix}, \begin{pmatrix} L_0(s_4) \\ M_0(s_4) \end{pmatrix} = \begin{pmatrix} 0 \\ 1 \end{pmatrix} \tag{31}$$

Again equating the coefficients of next lowest degree term of x ; (i.e. x^{s-1}) in Eq. (25) to zero, we have the following matrix equation:

$$(g_1(s+1))_{2 \times 2} \begin{pmatrix} L_1(s) \\ M_1(s) \end{pmatrix} + (g_2(s+1))_{2 \times 2} \begin{pmatrix} L_0(s) \\ M_0(s) \end{pmatrix} = 0 \tag{32}$$

where $g_1(s+1)$ and $g_2(s+1)$ are shown in appendix (55). On simplification of matrix Eq. (32), we find:

$$\begin{pmatrix} L_1(s_j) \\ M_1(s_j) \end{pmatrix} = - \begin{pmatrix} 0 & e_{12}^1(s_j) \\ e_{21}^1(s_j) & 0 \end{pmatrix} \begin{pmatrix} L_0(s_j) \\ M_0(s_j) \end{pmatrix} \tag{33}$$

$e_{12}^1(s_j)$ and $e_{21}^1(s_j)$ are defined in appendix (56). Now equating the coefficients of like powers of x^{s+k} in Eq. (25) to zero, we obtain the following recurrence relation:

$$\sum_{k=0}^{\infty} \left\{ (g_1(s_j+k+2))_{2 \times 2} \begin{pmatrix} L_{k+2}(s_j) \\ M_{k+2}(s_j) \end{pmatrix} + (g_2(s_j+k+1))_{2 \times 2} \begin{pmatrix} L_{k+1}(s_j) \\ M_{k+1}(s_j) \end{pmatrix} + (g)_{2 \times 2} \begin{pmatrix} L_k(s_j) \\ M_k(s_j) \end{pmatrix} \right\} = 0 \tag{34}$$

On simplification of recurrence relation of Eq. (34), we get the following relation:

$$\begin{pmatrix} L_{k+2}(s_j) \\ M_{k+2}(s_j) \end{pmatrix} = - \begin{pmatrix} 0 & g_{12}^k(s_j) \\ g_{21}^k(s_j) & 0 \end{pmatrix} \begin{pmatrix} L_{k+1}(s_j) \\ M_{k+1}(s_j) \end{pmatrix} - \begin{pmatrix} g_{11}^k(s_j) & 0 \\ 0 & g_{22}^k(s_j) \end{pmatrix} \begin{pmatrix} L_k(s_j) \\ M_k(s_j) \end{pmatrix};$$

$$k = 0, 1, \dots \tag{35}$$

where $g_{11}^k(s_j)$, $g_{12}^k(s_j)$, $g_{21}^k(s_j)$ and $g_{22}^k(s_j)$ are defined in appendix (57) and (58). Substituting $k = 0$, in Eq. (35) and on simplification we get:

$$\begin{pmatrix} L_2(s_j) \\ M_2(s_j) \end{pmatrix} = \begin{pmatrix} e_{11}^2(s_j) & 0 \\ 0 & e_{22}^2(s_j) \end{pmatrix} \begin{pmatrix} L_0(s_j) \\ M_0(s_j) \end{pmatrix} \tag{36}$$

Here $e_{11}^2(s_j)$ and $e_{22}^2(s_j)$ are defined in appendix (57). Again substituting $k = 1$, in Eq. (35), on simplification this provides us:

$$\begin{pmatrix} L_3(s_j) \\ M_3(s_j) \end{pmatrix} = - \begin{pmatrix} 0 & e_{12}^3(s_j) \\ e_{21}^3(s_j) & 0 \end{pmatrix} \begin{pmatrix} L_0(s_j) \\ M_0(s_j) \end{pmatrix} \quad (37)$$

$e_{12}^3(s_j)$ and $e_{21}^3(s_j)$ are defined in appendix (60). Again substituting $k = 2$, in Eq. (35) and after simplification this is written as:

$$\begin{pmatrix} L_4(s_j) \\ M_4(s_j) \end{pmatrix} = \begin{pmatrix} e_{11}^4(s_j) & 0 \\ 0 & e_{22}^4(s_j) \end{pmatrix} \begin{pmatrix} L_0(s_j) \\ M_0(s_j) \end{pmatrix} \quad (38)$$

$e_{11}^4(s_j)$ and $e_{22}^4(s_j)$ are defined in appendix (61). And continue so on in this manner, it may be explained that the matrix $(L_{2k}(s_j) \ M_{2k}(s_j))'$ has similar form to that $(g_1(s+k))_{2 \times 2}$ and $(L_{2k+1}(s_j) \ M_{2k+1}(s_j))'$ is alike to $(g_2(s+k))_{2 \times 2}$. Therefore, in general this is written as:

$$\begin{pmatrix} L_{2k}(s_j) \\ M_{2k}(s_j) \end{pmatrix} = \begin{pmatrix} e_{11}^{2k}(s_j) & 0 \\ 0 & e_{22}^{2k}(s_j) \end{pmatrix} \begin{pmatrix} L_0(s_j) \\ M_0(s_j) \end{pmatrix}; \quad (39)$$

$k = 1, 2, 3, \dots$

$$\begin{pmatrix} L_{2k+1}(s_j) \\ M_{2k+1}(s_j) \end{pmatrix} = - \begin{pmatrix} 0 & e_{12}^{2k+1}(s_j) \\ e_{21}^{2k+1}(s_j) & 0 \end{pmatrix} \begin{pmatrix} L_0(s_j) \\ M_0(s_j) \end{pmatrix}; \quad (40)$$

$k = 1, 2, 3, \dots$

where $e_{11}^{2k}(s_j)$, $e_{12}^{2k+1}(s_j)$, $e_{21}^{2k+1}(s_j)$ and $e_{22}^{2k}(s_j)$ are defined in appendix (62) to (65).

From Eqs. (36)–(40), we get

$$\begin{pmatrix} e_{11}^{2k}(s_j) & 0 \\ 0 & e_{22}^{2k}(s_j) \end{pmatrix} = o\left(\frac{1}{k}\right) \begin{pmatrix} A^* & 0 \\ 0 & B^* \end{pmatrix}; \quad k = 1, 2, 3, \dots \quad (41)$$

$$\begin{pmatrix} 0 & e_{12}^{2k+1}(s_j) \\ e_{21}^{2k+1}(s_j) & 0 \end{pmatrix} = o\left(\frac{1}{k}\right) \begin{pmatrix} 0 & A^* \\ B^* & 0 \end{pmatrix}; \quad (42)$$

$k = 1, 2, 3, \dots$

Due to Cullen [27], the matrix sequence $\{G_k\}$ in the complex field converges, $(\lim_{k \rightarrow \infty} G_k = G)$, if each of k component sequence converges. Introducing the above fact that both the matrices $\begin{pmatrix} e_{11}^{2k}(s_j) & 0 \\ 0 & e_{22}^{2k}(s_j) \end{pmatrix} \rightarrow 0$ and $\begin{pmatrix} 0 & e_{12}^{2k+1}(s_j) \\ e_{21}^{2k+1}(s_j) & 0 \end{pmatrix} \rightarrow 0$ as $k \rightarrow \infty$. This implies that the considered sequences in Eq. (24) are absolutely and uniformly convergent. Thus, the considered sequence in solution (24) becomes:

$$\begin{pmatrix} v \\ \theta \end{pmatrix} = \left\{ I - \begin{pmatrix} 0 & e_{12}^1(s_j) \\ e_{21}^1(s_j) & 0 \end{pmatrix} x + \begin{pmatrix} e_{11}^2(s_j) & 0 \\ 0 & e_{22}^2(s_j) \end{pmatrix} x^2 - \begin{pmatrix} 0 & e_{12}^3(s_j) \\ e_{21}^3(s_j) & 0 \end{pmatrix} x^3 + \dots \right\} \begin{pmatrix} L_0(s_j) \\ M_0(s_j) \end{pmatrix} x^{s_j}; \quad (43)$$

Here I is identity matrix of order two. Hence, the considered sequence in series Eq. (24) and the derived series are analytic function and having term-by-term differentiation.

Thus, general solution of Eq. (17) with the help of Eq. (43) via (24) is obtained as:

$$w(x, \tau) = \sum_{k=0}^{\infty} \left\{ \begin{aligned} & (H_{1k} e_{11}^{2k}(s_1) x^{s_1} + H_{2k} e_{11}^{2k}(s_2) x^{s_2}) \\ & + (H_{3k} e_{12}^{2k+1}(s_3) x^{s_3+1} + H_{4k} e_{12}^{2k+1}(s_4) x^{s_4+1}) \end{aligned} \right\} x^{2k-\frac{\gamma}{2}} \exp(i\Omega\tau) \quad (44)$$

$$\theta(x, \tau) = \sum_{k=0}^{\infty} \left\{ \begin{aligned} & (H_{1k} e_{21}^{2k+1}(s_1) x^{s_1+1} + H_{2k} e_{21}^{2k+1}(s_2) x^{s_2+1}) \\ & + (H_{3k} e_{22}^{2k}(s_3) x^{s_3} + H_{4k} e_{22}^{2k}(s_4) x^{s_4}) \end{aligned} \right\} x^{2k-\frac{\gamma}{2}} \exp(i\Omega\tau) \quad (45)$$

where H_{1k} , H_{2k} , H_{3k} and H_{4k} are arbitrary constants to be determined. Applying time harmonics and transformation from Eqs. (17) and (21) on the boundary conditions of Eq. (15) and (16), we obtain the transformed boundary conditions in non-dimensional form as:

$$\frac{dw}{dx} + \frac{m_5 w}{\tilde{\delta}_0 x} - i\Omega m_3 \theta = 0, \quad \theta = 0 \quad \text{at } x = \zeta \quad (46)$$

$$\frac{dw}{dx} + \frac{m_5 w}{\tilde{\delta}_0 x} - i\Omega m_3 \theta = -Q^*, \quad \frac{d\theta}{dx} - \frac{\gamma}{2x} \theta = 0 \quad \text{at } x = 1 \quad (47)$$

where $Q^* = \frac{i\Omega^{-1}}{\tilde{\delta}_0} Q$

Using Eqs. (44) and (45) in Eqs. (46) and (47), we obtain:

$$\begin{pmatrix} H_{1k} \\ H_{2k} \\ H_{3k} \\ H_{4k} \end{pmatrix} = \begin{pmatrix} e_{11} & e_{12} & e_{13} & e_{14} \\ e_{21} & e_{22} & e_{23} & e_{24} \\ e_{31} & e_{32} & e_{33} & e_{34} \\ e_{41} & e_{42} & e_{43} & e_{44} \end{pmatrix}^{-1} \begin{pmatrix} 0 \\ 0 \\ -Q^* \\ 0 \end{pmatrix} \quad (48)$$

where

$$\begin{aligned} e_{11} &= \left\{ (2k + s_1 + a^*) \frac{1}{\zeta} e_{11}^{2k}(s_1) + b^* \zeta e_{21}^{2k+1}(s_1) \right\} \zeta^{2k+s_1}; \\ e_{13} &= \left\{ (2k + s_3 + 1 + a^*) \zeta e_{12}^{2k+1}(s_3) + b^* e_{22}^{2k}(s_3) \right\} \zeta^{2k+s_3}; \\ e_{21} &= e_{21}^{2k+1}(s_1) \zeta^{2k+1+s_1}; \quad e_{23} = e_{22}^{2k}(s_3) \zeta^{2k+s_3}; \\ e_{31} &= (2k + s_1 + a^*) e_{11}^{2k}(s_1) + b^* e_{21}^{2k+1}(s_1); \\ e_{33} &= (2k + s_3 + 1 + a^*) e_{12}^{2k+1}(s_3) + b^* e_{22}^{2k}(s_3); \\ e_{41} &= \left(2k + s_1 + \frac{2-\gamma}{2} \right) e_{21}^{2k+1}(s_1); \\ e_{43} &= \left(2k + s_3 - \frac{\gamma}{2} \right) e_{22}^{2k}(s_3); \\ a^* &= (1 - 2\delta^2) \frac{\tilde{\alpha}_0}{\tilde{\delta}_0} - \frac{\gamma}{2}, \quad b^* = \frac{i\tilde{e}\Omega\tilde{\beta}_0\tilde{\tau}_1}{\tilde{\delta}_0} \end{aligned} \quad (49)$$

The elements $e_{12}, e_{22}, e_{32}, e_{42}$ are written from $e_{11}, e_{21}, e_{31}, e_{41}$ by replacing s_1 with s_2 , and the elements $e_{14}, e_{24}, e_{34}, e_{44}$ are written from $e_{13}, e_{23}, e_{33}, e_{43}$ by replacing s_3 with s_4 . Equations (44) to (48) represent the formal solution of the problem, which are boundary conditions of Eqs. (15) and (16). In this analysis, we represent periodic dynamic pressures as given by Keles and Tutuncu [4]. For periodic pressure, we consider the function $Q(\tau)$ as periodic dynamic pressure

$$Q = Q(\tau) = Q_0(1 - \cos \Omega\tau) \tag{50}$$

6 Validation of Results with Deductions

In this section, the deduction has been done for the validation of above analytical results for coupled and uncoupled functionally graded material viscothermoelastic and thermoelastic cylinders by comparing with available results in the literature.

6.1 Coupled Viscothermoelastic and Thermoelastic Functionally Graded Cylinders

In case, the thermal relaxation time has been vanished by taking ($\tau_0 = \tau'_0 = \tau_1 = 0$), the quantity m_3 and m_4 becomes $m_3 = \frac{i\Omega^{-1}\bar{\epsilon}\beta_0}{\delta_0}$ and $m_4 = \frac{\epsilon_T}{\bar{\epsilon}}i\Omega^{-1}\Omega^*\beta_0$. Again in case of coupled thermoelastic case, the relaxation time and viscoelastic parameters by taking ($\alpha_0 = \alpha_1 = \beta_0 = \tau_0 = \tau'_0 = \tau_1 = 0$), the terms m_3, m_4 and η^2 become $m_3 = i\Omega^{-1}\bar{\epsilon}$, $m_4 = -\frac{\epsilon_T}{\bar{\epsilon}}\Omega^*$ and $\eta^2 = \frac{\gamma}{4} - \bar{h}\gamma + 1$, so that Eqs. (22) and (23) reduce to:

$$\left\{ \nabla^2 + \left(\Omega^2 + \frac{1}{x^2} \left(\frac{\gamma^2}{4} - \bar{h}\gamma + 1 \right) \right) \right\} v - \bar{\epsilon} \left(\frac{d}{dx} + \frac{\gamma}{2x} \right) \theta = 0$$

$$\left\{ \nabla^2 - \left(\frac{\gamma^2}{4x^2} + i\Omega\Omega^* \right) \right\} \theta - i\Omega^3 \frac{\epsilon_T}{\bar{\epsilon}} \Omega^* \left(\frac{d}{dx} + \frac{1-\gamma/2}{x} \right) v = 0 \tag{51}$$

$$\begin{pmatrix} \tau_{xx} \\ \tau_{\theta\theta} \end{pmatrix} = -i\Omega x^{-\frac{3}{2}} \begin{pmatrix} \left(\frac{d}{dx} + \left\{ \bar{h} + \frac{i\Omega\gamma}{2} \right\} \frac{1}{x} \right) \bar{\epsilon} \\ \bar{h} \left(\frac{d}{dx} + \left\{ \frac{1}{\bar{h}} - \frac{\gamma}{2} \right\} \frac{1}{x} \right) \bar{\epsilon} \end{pmatrix} \begin{pmatrix} w \\ \theta \end{pmatrix} \tag{52}$$

The results of Eqs. (51) and (52) are consistent with Sharma et al. [15] in the case of transversely isotropic functionally graded cylinder for LS theory of generalized thermoelasticity.

6.2 Uncoupled Viscoelastic Functionally Graded Cylinders

Here when the media is considered either at isothermal or at adiabatic conditions, the situations are either at thermal

equilibrium or isentropic conditions. So that we have either $\epsilon_T = 0 = \tilde{\beta}_0$ or $T = 0$. Thus, the solutions of Eqs. (44) and (45) become:

$$w(x, \tau) = x^{-\frac{3}{2}} \sum_{k=0}^{\infty} \{ H_{1k} e_{11}^{2k}(s_1) x^{s_1} + H_{2k} e_{11}^{2k}(s_2) x^{s_2} \} x^{2k} \exp(i\Omega\tau) \tag{53}$$

$$\theta(x, \tau) = x^{-\frac{3}{2}} \sum_{k=0}^{\infty} \{ H_{1k} e_{21}^{2k+1}(s_1) x^{s_1} + H_{2k} e_{21}^{2k+1}(s_2) x^{s_2} \} x^{2k+1} \exp(i\Omega\tau) \tag{54}$$

7 Numerical Results and Discussion

To validate the analytical result of the formulation, the numerical simulations have been presented with the help of MATLAB software tools. Polymethyl methacrylate material has been taken for numerical computations whose physical data are given below with reference to Othman et al. [5] after approximation

$$\lambda = 5.16 \times 10^8 \text{ Nm}^{-2}, \quad \mu = 5.01 \times 10^8 \text{ Nm}^{-2},$$

$$\rho = 1190 \text{ kg m}^{-3}, \quad \alpha_T = 77 \times 10^{-6} \text{ K}^{-1},$$

$$\epsilon_T = 0.045, \quad \omega^* = 1.11 \times 10^{11} \text{ s}^{-1}, \quad T_0 = 773 \text{ K},$$

$$\delta^2 = 0.333, \quad C_e = 1400 \text{ J kg}^{-1} \text{ K}^{-1},$$

$$\hat{\alpha}_0 = \hat{\alpha}_1 = 0.05, \quad \tau_0 = 0.02, \quad \tau_1 = 0.03,$$

$$K = 0.19 \text{ W m}^{-1} \text{ K}^{-1}.$$

We simply solve the corresponding linear system of Eqs. (44), (45) and (48) by MATLAB software tools and estimate the results by the allowed error less than 10^{-6} . The errors in the results are negligibly small; hence, it is not taken into consideration. The numerical data we have taken only rounding off error in data up to six decimal places.

The numerical calculations have been carried out by choosing the ratio of inner radius to outer radius $\zeta = 2$ and radial distance $x = 1.5$ from the center of disk. The numerical computations for variation of temperature, displacement, radial and de-hoop stresses are demonstrated through Figs. 1, 2, 3 and 4 against time and Figs. 5, 6, 7 and 8 against normalized thickness. The temperature change, radial displacement and stresses are noted to vanish initially at $\tau = 0$, which agree with our assumption of the initial boundary conditions. Figures 1, 2, 3 and 4 represent the patterns of non-dimensional temperature, radial displacement and stresses of homogeneous ($\gamma = 0$) and non-homogeneous ($\gamma = 2.5, 5.0$) materials, due to the pressure $Q(\tau)$ with $\Omega = 1.0, Q_0 = \bar{\epsilon}$, respectively. It is observed from Fig. 1 that amplitudes of these quantities keep on interchanging with time for ($\gamma = 0, 2.5, 5.0$). The variation in magnitude of temperature is larger in

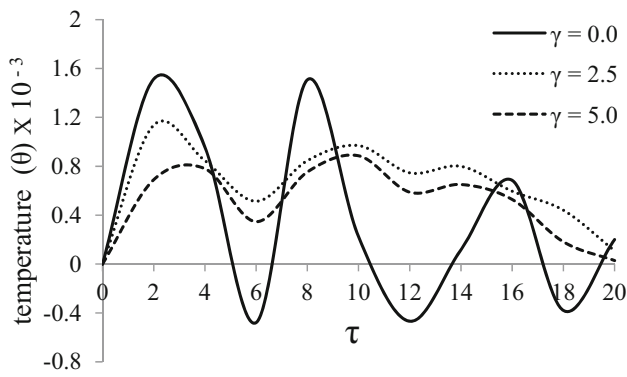


Fig. 1 Time history of temperature change (θ)

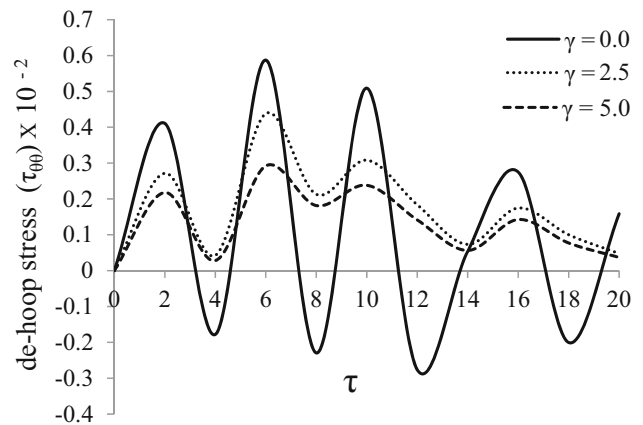


Fig. 4 Time history of de-hoop stress ($\tau_{\theta\theta}$)

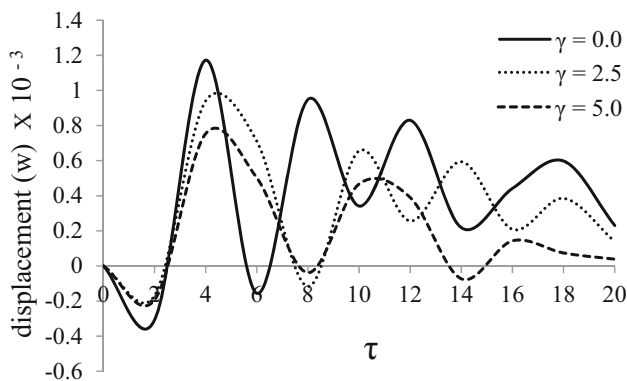


Fig. 2 Time history of radial displacement (w)

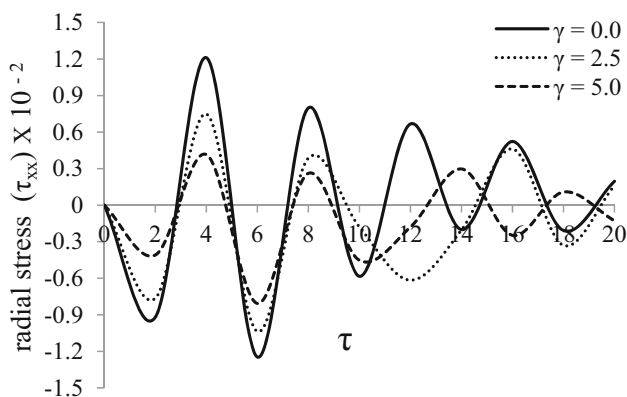


Fig. 3 Time history of radial stress (τ_{xx})

homogeneous case, i.e., ($\gamma = 0$) rather than non-homogeneous cases, i.e., ($\gamma = 2.5, 5.0$), and with the increase in time the variation of temperature decreases. It is noted from Fig. 2 (displacements against time) that the quantities go on interchanging with time and have larger variation at $\tau = 4.0$ for all the cases, and with the increase in value of time, the variation of amplitude decreases. It is revealed from Fig. 3 that the variations are sinusoidally decreasing with time. From Fig. 4, the variations have the highest peak

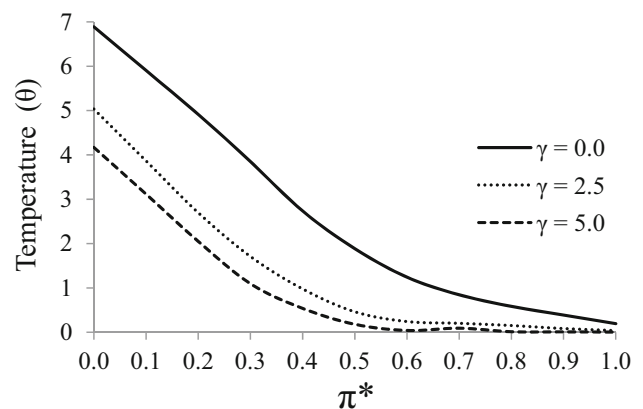


Fig. 5 Variation of temperature change (θ) against normalized thickness (π^*)

at $\tau = 6.0$, and with the increase in the value of τ , the variation of amplitude of de-hoop stresses for different values of γ decreases. This is to be noted that the amplitude of all the figures shows larger variation in homogeneous material rather than non-homogeneous materials.

Figures 5, 6, 7 and 8 display the variations of temperature change (θ), displacement (w), radial stress (τ_{xx}) and de-hoop stress ($\tau_{\theta\theta}$) against normalized thickness ($\pi^* = \frac{x-1}{\xi-1}$; $\xi \neq 1$) (here $0 \leq \pi^* \leq 1$) for different values of γ . From Fig. 5, the temperature change decreases with the increasing values of π^* . The amplitude of temperature profile decreases due to inhomogeneity parameter and varies according to $\gamma = 5.0 < 2.0 < 0.0$. From Fig. 6, variation of displacement (w) increases sharply to attain its maximum value between $0.3 < \pi^* < 0.5$ and decreases to become ultimately asymptotic with the increasing value of (π^*). From Fig. 7, variation of radial stress (τ_{xx}) shows initially compressive behavior, peaking at $\pi^* = 0.3$, and on further increase in π^* , variations decrease. From Fig. 8, the de-hoop stress shows the tensile behavior attains the

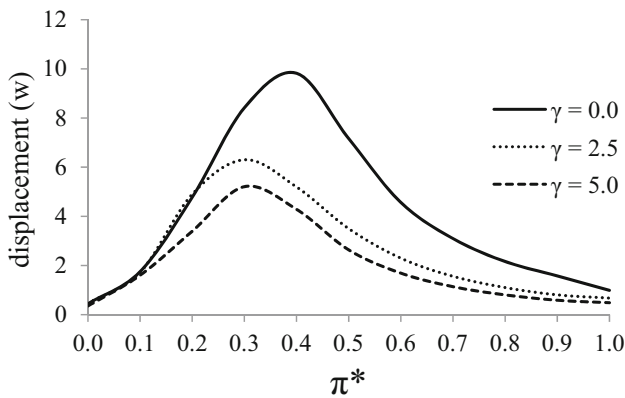


Fig. 6 Variation of radial displacement (w) against normalized thickness (π^*)

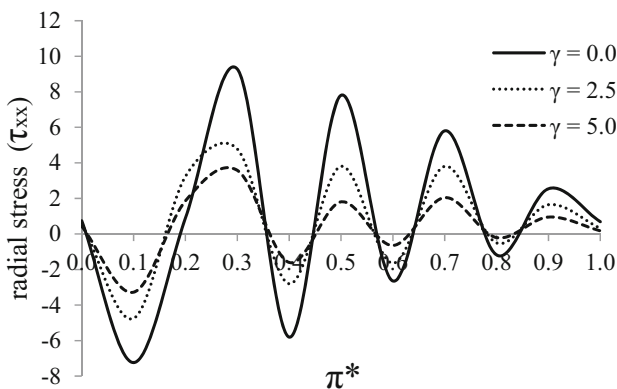


Fig. 7 Variation of radial stress (τ_{xx}) against normalized thickness (π^*)

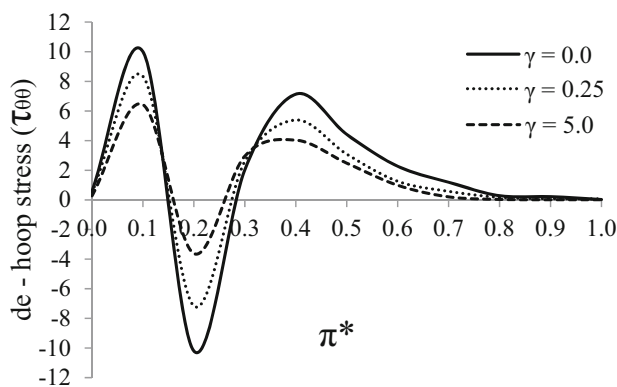


Fig. 8 Variation of de-hoop stress ($\tau_{\theta\theta}$) against normalized thickness (π^*)

maximum magnitude at $\pi^* = 0.1$ and becomes compressive at $\pi^* = 0.2$, and with the increase in π^* , variations decrease and die out. From all the figures, it is concluded that the variations are larger for homogeneous material, i.e. ($\gamma = 0$) in contrast with the smaller variations for non-homogeneous materials, i.e. ($\gamma = 2.5, 5.0$). It may also be

observed that deformation and stress development may be monitored (increased/decreased) as per requirement by increasing or decreasing the value of grading index γ .

8 Concluding Remarks

The extended power series solution of matrix Fröbenius method has been applied successfully to represent the axisymmetric forced vibrations of viscothermoelastic hollow cylinders under dynamic pressure. With the assistance of non-homogeneity grading parameter, the twist (displacement), change in temperature and development of stress have been examined as per requirement. Here the approach is well-organized and useful to represent that the closed-form analytical solutions due to non-homogeneity grading parameter for generalized theories of viscothermoelasticity have considerable effect on forced vibration characteristics. Significant effects of thermal and mechanical relaxation times have been observed on viscothermoelastic stresses, displacement and temperature distributions. As the grading parameter increases, the variation is noted to be lower. The results are consistent with [4] in the absence of thermal and viscous effects.

Appendix

$$g_1(s+1) = \begin{pmatrix} (s+1)^2 - \eta^2 & 0 \\ 0 & \left((s+1)^2 - \frac{\gamma^2}{4} \right) \end{pmatrix}; \tag{55}$$

$$g_2(s+1) = \begin{pmatrix} 0 & A^* \left(s+1 + \frac{\gamma}{2} \right) \\ B^* \left(s+1 + \frac{2-\gamma}{2} \right) & 0 \end{pmatrix};$$

$$e_{12}^1(s_j) = A^* \frac{(s_j + \frac{2+\gamma}{2})}{(s+1)^2 - \eta^2}, \quad e_{21}^1(s_j) = B^* \frac{(s_j + \frac{4-\gamma}{2})}{(s+1)^2 - \frac{\gamma^2}{4}}; \tag{56}$$

$j = 1, 2, 3, 4;$

$$g_{11}^k(s_j) = \frac{i\Omega}{\tilde{\delta}_0 \left((s_j + k + 2)^2 - \eta^2 \right)}, \tag{57}$$

$$g_{22}^k(s_j) = \frac{\Omega^* \Omega^2 \tilde{\tau}_0}{\left((s_j + k + 2)^2 - \frac{\gamma^2}{4} \right)};$$

$$g_{12}^k(s_j) = \frac{A^* \left(s_j + k + \frac{2+\gamma}{2} \right)}{\left((s_j + k + 2)^2 - \eta^2 \right)}, \tag{58}$$

$$g_{21}^k(s_j) = \frac{B^* \left(s_j + k + \frac{4-\gamma}{2} \right)}{\left((s_j + k + 2)^2 - \frac{\gamma^2}{4} \right)};$$

$$\begin{aligned} e_{11}^2(s_j) &= g_{12}^0(s_j) e_{21}^1(s_j) - g_{11}^0(s_j), & e_{22}^2(s_j) &= g_{21}^0(s_j) \\ & e_{12}^1(s_j) - g_{22}^0(s_j) \end{aligned} \tag{59}$$

$$\begin{aligned} e_{12}^3(s_j) &= g_{12}^1(s_j) e_{22}^2(s_j) - g_{11}^1(s_j) e_{12}^1(s_j), \\ e_{21}^3(s_j) &= g_{21}^1(s_j) e_{11}^2(s_j) - g_{22}^1(s_j) e_{21}^1(s_j) \end{aligned} \tag{60}$$

$$\begin{aligned} e_{11}^4(s_j) &= g_{12}^2(s_j) e_{21}^3(s_j) - g_{11}^2(s_j) e_{11}^2(s_j), \\ e_{22}^4(s_j) &= g_{21}^2(s_j) e_{12}^3(s_j) - g_{22}^2(s_j) e_{21}^2(s_j) \end{aligned} \tag{61}$$

$$e_{11}^{2k}(s_j) = g_{12}^{2k-2}(s_j) e_{21}^{2k-1}(s_j) - g_{11}^{2k-2}(s_j) e_{11}^{2k-2}(s_j); \tag{62}$$

$$e_{22}^{2k}(s_j) = g_{21}^{2k-2}(s_j) e_{12}^{2k-1}(s_j) - g_{22}^{2k-2}(s_j) e_{21}^{2k-1}(s_j); \tag{63}$$

$$e_{12}^{2k+1}(s_j) = g_{12}^{2k-1}(s_j) e_{22}^{2k}(s_j) - g_{11}^{2k-1}(s_j) e_{12}^{2k-1}(s_j); \tag{64}$$

$$e_{21}^{2k+1}(s_j) = g_{21}^{2k-1}(s_j) e_{11}^{2k}(s_j) - g_{22}^{2k-1}(s_j) e_{21}^{2k-1}(s_j) \tag{65}$$

References

1. Chen WT (1966) On some problems in spherically isotropic elastic materials. *J Appl Mech* 33:539–546
2. Honarvar F, Sinclair AN (1996) Acoustic wave scattering from transversely isotropic cylinders. *J Acoust Soc Am* 100:57–63
3. Dai H-L, Rao Y-N, Jiang H-J (2013) Thermoelastic dynamic response for a long functionally graded hollow cylinder. *J Compos Mater* 47:315–325
4. Keles I, Tutuncu N (2011) Exact analysis of axisymmetric dynamic response of functionally graded cylinders (or disks) and spheres. *J Appl Mech*. <https://doi.org/10.1115/1.4003914>
5. Othman MIA, Ezzat MA, Zaki SA, El-Karamany AS (2002) Generalized thermo-viscoelastic plane waves with two relaxation times. *Int J Eng Sci* 40:1329–1347
6. Flügge W (1975) *Viscoelasticity*. Springer, Berlin
7. Hunter C, Sneddon I, Hill R (1960) *Visco-elastic waves in progress in solid mechanics*. Wiley, New York
8. Lord HW, Shulman Y (1967) A generalized dynamical theory of thermoelasticity. *J Mech Phys Solids* 15:299–309
9. Green AE, Lindsay KA (1972) *Thermoelasticity*. *J Elast* 2:1–7
10. Sharma JN, Othman MIA (2007) Effect of rotation on generalized thermo-viscoelastic Rayleigh–Lamb waves. *Int J Solids Struct* 44:4243–4255
11. Sharma JN, Singh H, Sharma YD (2011) Modeling of thermoelastic damping and frequency shift of vibrations in a transversely isotropic solid cylinder. *Multidiscipl Model Mater Struct* 7:245–265

12. Sharma JN, Kumari N, Sharma KK (2013) Diffusion in a generalized thermoelastic solid in an infinite body with cylindrical cavity. *Proc Natl Acad Sci India Sect A* 83:353–364
13. Sharma JN, Sharma DK, Dhaliwal SS (2012) Three-dimensional free vibration analysis of a viscothermoelastic hollow sphere. *Open J Acoust* 2:12–24
14. Sharma JN, Sharma DK, Dhaliwal SS (2013) Free vibration analysis of a rigidly fixed viscothermoelastic hollow sphere. *Indian J Pure Appl Math* 44:559–586
15. Sharma JN, Sharma PK, Mishra KC (2014) Analysis of free vibrations in axisymmetric functionally graded thermoelastic cylinders. *Acta Mech* 225:1581–1594
16. Sharma DK, Sharma JN, Dhaliwal SS, Walia V (2014) Vibration analysis of axisymmetric functionally graded viscothermoelastic spheres. *Acta Mech Sin* 30:100–111
17. Xin L, Dui G, Yang S, Zhang J (2014) An elasticity solution for functionally graded thick walled tube subjected to internal pressure. *Int J Mech Sci* 89:344–349
18. Xin L, Dui G, Yang S (2015) Solution for behavior of a functionally graded thick-walled tube subjected to mechanical and thermal loads. *Int J Mech Sci* 98:70–79
19. Tripathi JJ, Kedar GD, Deshmukh KC (2015) Generalized thermoelastic diffusion problem in a thick circular plate with axisymmetric heat supply. *Acta Mech* 226:2121–2134
20. Khanna A, Kaur N (2016) Theoretical study on vibration of non-homogeneous tapered visco-elastic rectangular plate. *Proc Natl Acad Sci India Sect A* 86:259–266
21. Sharma JN, Sharma PK, Mishra KC (2016) Dynamic response of functionally graded cylinders due to time-dependent heat flux. *Meccanica* 51:139–154
22. Xin L, Lu W, Yang S, Ju C, Dui G (2016) Influence of linear work hardening on the elastic–plastic behavior of a functionally graded thick walled tube. *Acta Mech* 227(8):2305–2321
23. Sharma DK (2016) Free vibrations of homogenous isotropic viscothermoelastic spherical curved plates. *J Appl Sci Eng* 19:135–148
24. Sharma N (2017) Circumferential waves in transversely isotropic thermoelastic spherical curved plates. *Proc Natl Acad Sci India Sect A* 87:57–72
25. Xin L, Dui G, Pan Li Y (2018) A revisiting of the elasticity solution for a transversely isotropic functionally graded thick-walled tube on the Mori–Tanaka method. *Acta Mech* 229(6):2703–2717
26. Tomantschger KW (2002) Series solutions of coupled differential equations with one regular singular point. *J Comput Appl Math* 140:773–783
27. Cullen CG (1990) *Matrices and linear transformations*, 2nd edn. Dover Publications, New York
28. Pierce AD (1981) *Acoustics: an introduction to its physical principles and applications*. McGraw-Hill Book Co, New York
29. Dhaliwal RS, Singh A (1980) *Dynamic coupled thermo elasticity*. Hindustan Publishing Corporation, New Delhi
30. Neuringer JL (1978) The Frobenius method for complex roots of the indicial equation. *Int J Math Educ Sci Technol* 9:71–77

Publisher’s Note Springer Nature remains neutral with regard to jurisdictional claims in published maps and institutional affiliations.